Supplementary Materials

Methods

Wrist-worn EDA Biosensors

Sympathetic postganglionic fibers innervate eccrine sweat glands and their activity is reflected in measurable changes in skin conductance at the surface[1]. Therefore, modulation in skin conductance, or more generally speaking, in electrodermal activity (EDA), is a unique parameter that reflects purely sympathetic activity without parasympathetic antagonism[1-4]. The design and validation of the wrist-worn EDA biosensor has been described in detail in an earlier publication[5]. Briefly, the sensor measures exosomatic skin conductance by applying direct current to the stratum corneum of the epidermis beneath measuring electrodes. To achieve a wide dynamic range of skin conductance measurements, the analog conditioning circuitry utilizes non-linear feedback automatic bias control with low-power operational amplifiers. The sensor module also contains a tri-axis accelerometer for measurements of physical activity (actigraphy). All the electronic components were integrated into a wristband made out of terrycloth for comfortable and inconspicuous use. We used disposable Ag/AgCl disc electrodes with contact areas of 1.0 cm^2 for our recordings as recommended in the literature[6]. The electrodes were dry; no gel was used. We use the ventral side of the distal forearms as recording sites as placement of electrodes on the forearm are less susceptible to motion artifacts and highly correlated to palmar recordings[5]. Each recording session lasted approximately 24 hours and batteries were replaced daily.

EDA Analysis

Raw EDA recordings were low-pass filtered (Hamming window, length = 1025, 3 Hz) to reduce motion artifacts and the filtered signals were used in all subsequent processing. We defined an EDA response as an increase greater than two SD above the baseline. To calculate the ictal EDA parameters, the segmented recordings were low-pass filtered (Hamming window, length = 1025, 0.01 Hz) to obtain the tonic component of EDA. The baseline was computed as the mean level over the entire 60 minutes pre-ictal period. Response latency was measured as the time from EEG seizure onset to the moment the filtered EDA signal exceeded two standard deviations (SD) above the pre-ictal baseline (EDA response onset). We quantified the magnitude of seizure-induced sympathetic activation by the peak amplitude of EDA response and area under the EDA response curve. EDA response amplitude was determined as the difference between the response peak and pre-ictal baseline. Response end time was established as the time when the EDA response fell below 90% of the EDA peak amplitude. The area under the EDA response curve was calculated by integrating the EDA signal from the EDA response onset to the end time after subtracting the baseline. Area under the rising portion was taken as the integral from the EDA response onset to the peak response. The natural log-transformation was applied to all area calculations as the formation of the sum of products generates a value that increases and decreases in an exponential manner.

ECG Analysis: Time-frequency Mapping of Heart Rate Variability

To assess parasympathetic activity, we performed time-frequency mapping of heart rate variability. Heart rate variability, a measure of fluctuations in the interval

between normal heartbeats mediated by autonomic inputs to the sinoatrial node, is an established measure of cardiac autonomic function[7, 8]. Vagal modulation can be quantified by analyzing oscillations at respiratory frequencies (also known as respiratory sinus arrhythmia) that are mediated solely by the parasympathetic system and are abolished by atropine infusion[9, 10].

All ECG recordings were analyzed using custom written software in MATLAB (MathWorks Inc., Natick, MA). ECG recordings were processed to remove noise as described by De Chazal and colleagues[11]. Baseline wander was removed by subtracting an estimate of the baseline obtained by two median filters. Power-line and high-frequency noise was then removed from the baseline-corrected ECG using a 12-tap low-pass filter (35 Hz) with equal ripple in the pass and stop bands. For each seizure, the corresponding peri-ictal filtered ECG signal from 60 minutes prior EEG seizure onset up to 120 min afterwards was segmented. The inter-beat interval (RRI) time series was formed by first employing automated QRS detecting using filter banks[12] and then manually examining the results to correct for false positives and missed beats. To remove artifacts such as ectopic beats, the RRI signal was filtered using the non-causal of variable threshold algorithm[13] with a tolerance of 20%. Next, the RRI signal was interpolated using a cubic spline at 4 Hz to obtain a uniformly sampled time series. The time profile of heart rate alterations (Figure 4A and 4B) was computed as $60/\overline{\mathrm{RRI}}$ with a one-minute sliding window with no overlap that was applied to the pre- and post-ictal segments.

For time-frequency analysis, baseline non-stationarities of the RRI series were removed by a detrending method based on a smoothness priors approach[14] with the

smoothing parameter $\lambda = 10$. The detrended RRI series was converted into an analytical signal using the Hilbert transform to remove negative frequencies. The smoothed pseudo Wigner-Ville (SPWV) time-frequency distribution with 1024 frequency bins was then computed using the analytical signal. We used a rectangular window (length = 121) for time-domain smoothing and a Gaussian window for frequency smoothing (length = 127). The parasympathetic mediated high frequency spectral component (HF) was extracted from the SPWV distribution by integrating the spectral powers between 0.15 and 0.4 Hz. The time profile of HF power alterations (Figure 4A and 4B) was obtained using a one-minute moving average window with no overlap that was applied to the pre- and post-ictal segments. The impact on parasympathetic function was measured as the maximal percentage change in HF power during the post-ictal period compared to the pre-ictal baseline. Pre-ictal baseline HF_{baseline} was determined by taking the mean value over the 30 minute period right before EEG seizure onset. The minimum HF power level HF_{min} was also determined from the 30 minute post-ictal period. The maximum percentage change in HF power ΔHF_{max} was defined as:

$$\Delta HF_{\text{max}} = \frac{HF_{\text{min}} - HF_{\text{baseline}}}{HF_{\text{baseline}}} \times 100\%$$

References

1. Critchley HD. Electrodermal responses: what happens in the brain. The Neuroscientist 2002;8:132-142.
2. Venables PH. Autonomic activity. Ann N Y Acad Sci 1991;620:191-207.
3. Wallin BG. Sympathetic nerve activity underlying electrodermal and cardiovascular reactions in man. Psychophysiology 1981;18:470-476.
4. Boucsein W. Electrodermal Activity. New York: Plenum Press, 1992.
5. Poh MZ, Swenson NC, Picard RW. A wearable sensor for unobtrusive, long-term assessment of electrodermal activity. IEEE Trans Biomed Eng 2010;57:1243-1252.
6. Fowles DC, Christie MJ, Edelberg R, Grings WW, Lykken DT, Venables PH. Committee report. Publication recommendations for electrodermal measurements. Psychophysiology 1981;18:232-239.
7. Stein P, Kleiger M. Insights from the study of heart rate variability. Annu Rev Med 1999;50:249-261.
8. Malik M, Thomas Bigger J, John Camm A, et al. Heart rate variability standards of measurement, physiological interpretation, and clinical use. Eur Heart J 1996;17:354-381.
9. Pomeranz B, Macaulay RJ, Caudill MA, et al. Assessment of autonomic function in humans by heart rate spectral analysis. Am J Physiol 1985;248:H151-153.
10. Akselrod S, Gordon D, Ubel F, Shannon D, Barger A, Cohen RJ. Power spectrum analysis of heart rate fluctuation: a quantitative probe of beat-to-beat cardiovascular control. Science 1981;213:220-222.
11. De Chazal P, O'Dwyer M, Reilly RB. Automatic classification of heartbeats using ECG morphology and heartbeat interval features. IEEE Trans Biomed Eng 2004;51:1196-1206.
12. Afonso VX, Tompkins WJ, Nguyen TQ, Luo S. ECG beat detection using filter banks. IEEE Trans Biomed Eng 1999;46:192-202.
13. Vila J, Palacios F, Presedo J, Fernandez-Delgado M, Felix P, Barro S. Time-frequency analysis of heart-rate variability. IEEE Eng Med Biol Mag 1997;16:119-126.
14. Tarvainen MP, Ranta-Aho PO, Karjalainen PA. An advanced detrending method with application to HRV analysis. IEEE Trans Biomed Eng 2002;49:172-175.
15. Lhatoo SD, Faulkner HJ, Dembny K, Trippick K, Johnson C, Bird JM. An electroclinical case-control study of sudden unexpected death in epilepsy. Ann Neurol 2010;68:787-796.

Supplementary Tables

Table e-1. Clinical characteristics of patients

Patient no./sex	Age/ epilepsy duration [years]	EEG seizure focus	MRI findings	Seizure frequency	AEDs	Duration of monitoring	Seizures included
1/m	15/13.5	Right>left posterior quadrant	Right occipital resection cavity (history of glioma)	2-4 CPS/week; 3 GTCS in life	LEV, LTG, MT, OXC	3 nights	2 CPS, 1 GTCS
2/m	17/1	Bifrontal	Frontal meningioma	1 GTCS/month	VPA	6 nights	4 GTCS
3/m	20/3	Left frontotemporal	Normal	2-3 CPS/week; 0.5 GTCS/month	CBZ, LEV	5 nights	1 CPS, 2 GTCS
4/m	9/9	Left frontotemporal	History of right thalamic hemorrhage	0.1-2 CPS/month	LTG, TGB, VPA	4 nights	1 GTCS
5/f	11/7	Multifocal	N.A.	N.A.	LEV, PHT, VPA	4 nights	2 CPS, 3 GTCS
6/m	16/15	Left frontotemporal	Normal	1-2 CPS/month; 2 GTCS/year	GBP, LOR, LTG, ZNS	5 nights	1 GTCS
7/m	13/N.A.	Right central	Right frontoparietal dysplasia	N.A.	DIA, LTG, PHT, TPM	4 nights	6 CPS
8/m	13/8	Left frontotemporal	Absence of corpus collosum, dysmorphic ventricles, bifrontal transmantle gray matter heterotopia, small pituitary gland	1-2 CPS/month; 1-2 GTCS/year	CBZ, LTG	5 nights	5 CPS
9/f	6.5/3	Left hemisphere	N.A.	3 CPS/day	CBZ, LTG	5 nights	4 CPS
10/m	3/1	Multifocal	Normal	1-2 CPS/week; 4 GTCS in life	CLN, LEV, LTG, VPA	4 nights	1 CPS
11/f	9/5	Left temporal	Normal	2-3 CPS/week	LEV, VPA	4 nights	1 CPS

AED antiepileptic drugs; CBZ carbamazepine; CLN clonazepam; CPS complex-partial seizure; DIA diazepam; GBP gabapentin; GTCS secondarily generalized tonic-clonic seizure; LEV levetiracetam; LOR lorazepam; LTG lamotrigine; MT melatonin; MRI magnetic resonance imaging; N.A. information not available; OXC oxcarbazepine; PHT phenytoin; TPM topiramate; VPA valproic acid; ZNS zonisamide

Table e-2. Summary of seizure-related EDA responses for individual patients

	GTCS			CPS		
Patient No.	**Proportion with EDA response***	**Amplitude of EDA response (μS)**	**Duration of EDA response (min)**	**Proportion with EDA response***	**Amplitude of EDA response (μS)**	**Duration of EDA response (min)**
1	1/1	20.95	40.72	2/2	0.57 ± 0.42	2.91 ± 0.98
2	4/4	17.03 ± 3.45	21.97 ± 5.56	n/a	n/a	n/a
3	2/2	21.90 ± 16.41	54.51 ± 41.79	1/1	0.43	2.01
4	1/1	3.93	21.24	n/a	n/a	n/a -
5	3/3	10.61 ± 2.82	12.87 ± 2.06	2/2	10.25 ± 8.24	9.32 ± 2.40
6	1/1	15.59	89.52	n/a	n/a	n/a
7	n/a	n/a	n/a	5/6	4.47 ± 1.97	12.26 ± 3.01
8	n/a	n/a	n/a	5/5	7.26 ± 1.99	13.85 ± 3.45
9	n/a	n/a	n/a	3/4	2.74 ± 0.35	18.94 ± 5.49
10	n/a	n/a	n/a	0/1	n/a	n/a
11	n/a	n/a	n/a	1/1	2.59	88.80

*Defined as an increase greater than 2 SD above the baseline.

Supplementary Figures

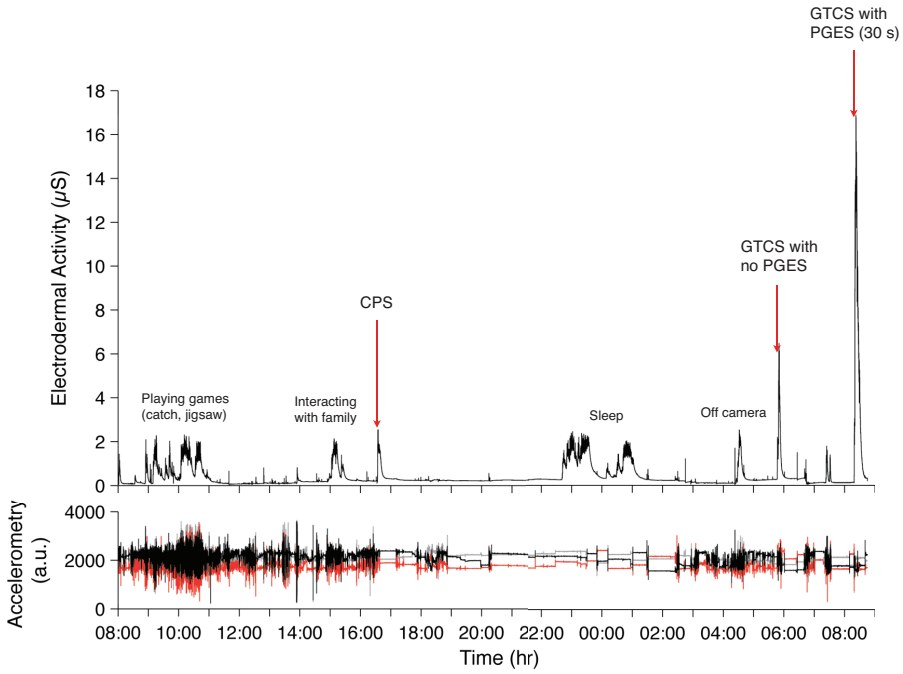

Figure e-1. Example of a 24-hour electrodermal activity (EDA) recording. Three seizures occurred during the recording period and each was associated with a varying amount of increase in EDA.

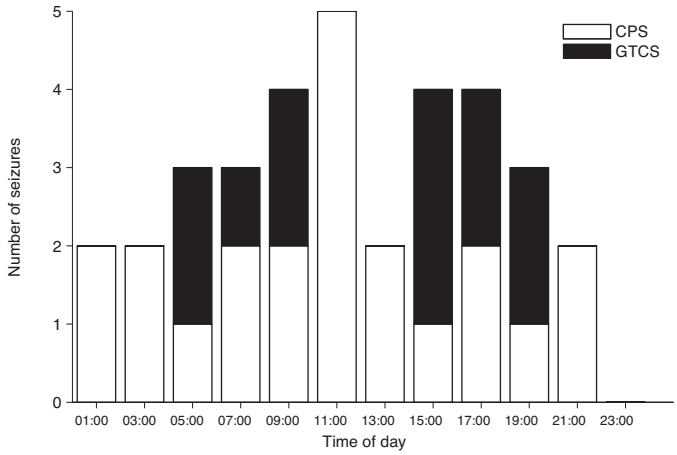

Figure e-2. Histogram of the onset times for the complex partial seizures (CPS) and secondarily generalized tonic-clonic seizures (GTCS) in this study. The occurrence times for both seizure types were distributed throughout the day and night.

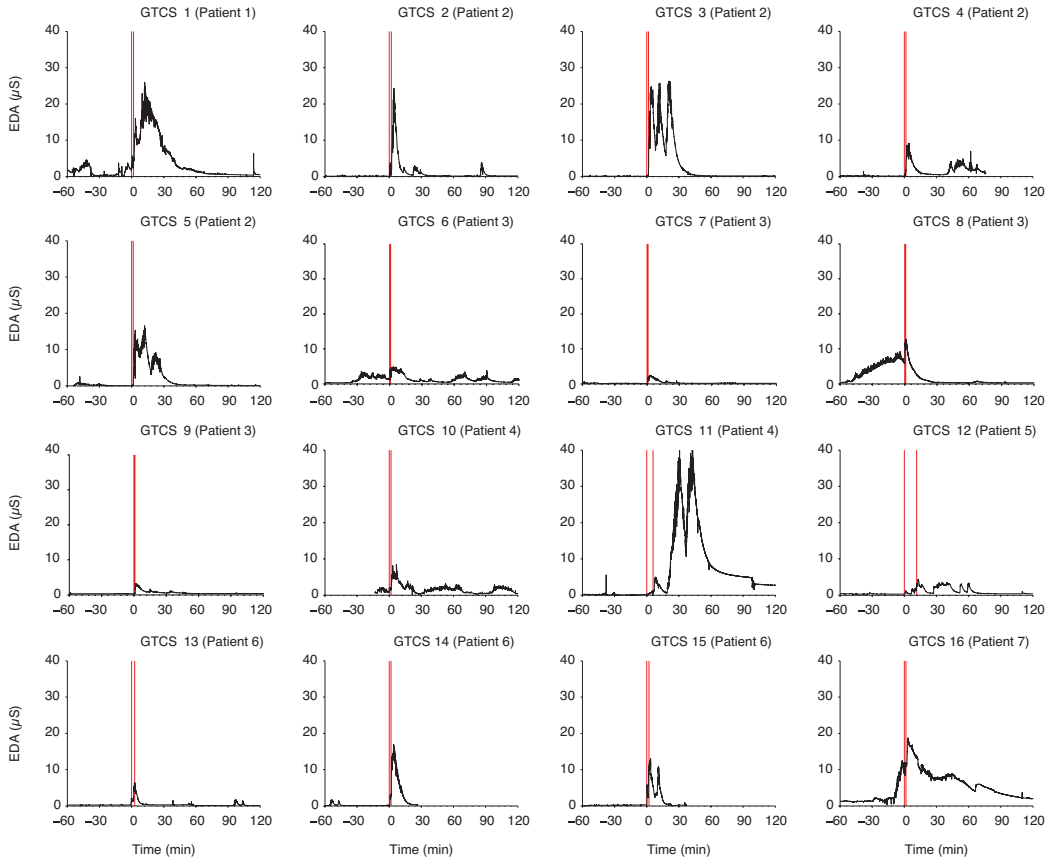

Figure e-3. Peri-ictal EDA recordings of individual GTCS. The rise in EDA typically occurs during the GTCS and reaches maximum during the post-ictal phase. Red lines denote seizure onset and offset.

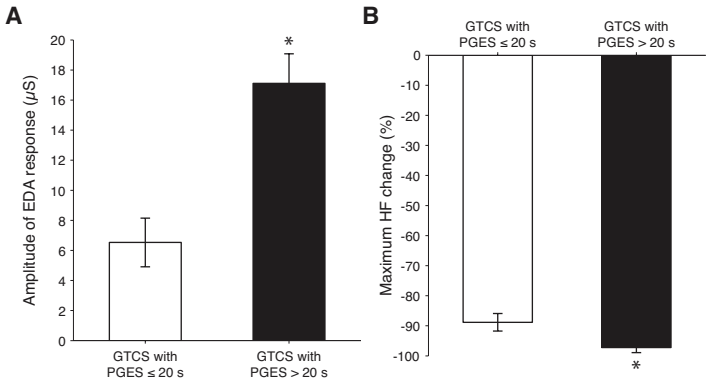

Figure e-4. Binary outcome analysis for prolonged post-ictal EEG suppression (PGES) in generalized tonic-clonic seizures (GTCS) We divided the convulsive seizures into lower and higher SUDEP risk groups to assess the difference in autonomic impact between the two groups. Lhatoo et al. reported that the odds ratio analysis of all seizures (both CPS and GTCS) indicated significantly elevated odds of SUDEP with PGES durations > 50 seconds. However, when only GTC seizures were considered, PGES durations > 20 seconds were also associated with significant elevations of odds ratios for SUDEP[15]. Thus 20 seconds suppression duration served as our threshold for grouping the seizures (repeated analysis using a 50 second threshold did not change the outcome). **(A)** GTCS with prolonged PGES (> 20 seconds) had a higher EDA response amplitude ($p = 0.01$; Mann-Whitney-Wilcoxon test [MWW]). **(B)** The maximum percentage decrease in HF power was greater in GTCS with higher prolonged PGES ($p < 0.05$; MWW).